Diffusion-Trapped Airy Beams in Photorefractive Media

Shu Jia, Joyce Lee, and Jason W. Fleischer

Department of Electrical Engineering and Princeton Institute for the Science and Technology of Materials, Princeton University, Princeton, New Jersey, 08544 USA

Georgios A. Siviloglou and Demetrios N. Christodoulides

College of Optics/CREOL, University of Central Florida Orlando, Florida, 32816 USA

(Received 9 December 2009; revised manuscript received 4 May 2010; published 24 June 2010)

We report the first experimental observation of self-trapped Airy beams in a nonlinear medium. As opposed to screening or photovoltaic spatial solitons, this new class of self-localized beams owes its existence to carrier diffusion effects. The asymmetric action of two-wave mixing supports the asymmetric intensity profile of the Airy states, with a balance that is independent of the beam intensity (unlike solitons). Further, the self-trapped wave packets self-bend during propagation at an acceleration rate that is independent of the thermal energy associated with the diffusive nonlinearity.

DOI: 10.1103/PhysRevLett.104.253904 PACS numbers: 42.70.Nq, 42.65.Jx, 78.20.Mg

The recent demonstration of optical Airy beams [1,2] has triggered a resurgence of interest in nondiffracting beam propagation. Like Bessel beams [3], Airy functions are exact solutions to the paraxial wave equation, are infinitely wide in the transverse direction, and are self-healing. Unlike other such beams, Airy beams are asymmetric and accelerate freely [1]. This curved trajectory, first noted within the framework of quantum mechanics by Berry and Balazs [4], has found immediate applications in optics, with interest ranging from optical trapping [5] and plasma waveguiding [6] to tomography [7] and frequency generation [8]. In practice, however, all nondiffracting beams must be truncated, to keep the energy finite. Such truncated beams eventually diffract and lose their unique structure and properties. Hence, it is important to identify physical mechanisms that could allow these highly localized wave packets to propagate in a true diffraction-free manner.

Nonlinear media naturally suggest themselves, as it is well known that self-focusing can counteract the effects of dispersion and diffraction [9]. For example, the nonlinear index change due to photoexcited charge carriers in photorefractive media, e.g., through screening [10–12] or photovoltaic effects [13,14], can lead to beam self-trapping and the formation of solitons. These invariant beams are usually symmetric, due to the even (second-order) nature of diffraction, and the typical nonlinear responses are local and conservative. Indeed, more complex responses, such as the gradient-sensitive diffusion nonlinearity [15], usually trigger a whole different class of instability and dynamics. For example, the nonlocal and nonconservative action of diffusion can cause energy exchange among spectral components, leading to two-wave mixing, beam fanning, and self-bending [16–18]. As a result, it has been commonly assumed that the diffusion nonlinearity cannot cause a beam to self-trap. On the other hand, the highly asymmetric action suggests that invariant propagation may be possible using highly asymmetric beams.

The prospect of observing a diffusion-trapped exponentially contained Airy wave packet in nonlinear photorefractive media was first proposed in Ref. [19]. In this Letter, we experimentally confirm this prediction and demonstrate that these wave packets self-bend during propagation at a rate that happens to be independent of the thermal energy k_BT. Further, we give direct evidence that internal wave mixing between the components underlies the self-localization process.

Before we present our experimental results, we will briefly outline some of the theoretical aspects associated with diffusion-trapped Airy states in photorefractive media. Starting from the Kukhtarev-Vinetskii model [15], the diffusion space-charge field $\vec{E}_{\rm sc}$ arising from an optical illumination intensity I can be determined from $\vec{E}_{\rm sc} = -(k_BT/e)\nabla I(I + I_d)^{-1}$ where k_BT is the thermal energy and e is the electron charge. I_d is the so-called dark irradiance that phenomenologically accounts for the rate of thermally generated electrons and will be neglected here, since in our work $I \gg I_d$. Given that our experiments were conducted in strontium barium niobate crystals ($Sr_{0.75}Ba_{0.25}Nb_2O_6$), we will subsequently focus our discussion on this material. The diffraction dynamics of a planar beam propagating along the a axis of this uniaxial crystal are governed by [19]

$$i\frac{\partial E}{\partial z} + \frac{1}{2k}\frac{\partial^2 E}{\partial x^2} + \frac{kn^2 r_{\rm eff} k_B T}{2e}\frac{(\partial|E|^2/\partial x)}{|E|^2}E = 0. \qquad (1)$$

In Eq. (1), n is the effective refractive index of the medium, $k = \omega n/c$ is the optical wave number, and E is the optical field envelope. $r_{\rm eff}$ stands for the electro-optic coefficient involved and the x coordinate coincides with the optical c axis. In the strontium barium niobate (SBN) configuration, for extraordinarily polarized waves $r_{\rm eff} = r_{33}$ while for

ordinarily polarized waves $r_{\text{eff}} = r_{13}$. In all cases, the beams are planar, e.g., diffraction takes place only along x. Under these conditions, a diffusion-trapped Airy state is possible and is given by [19]

$$E = E_0 \mathrm{Ai}(\varepsilon\eta + 4\gamma^2)\exp(-2\gamma\eta)\exp\{i[(\varepsilon\eta\xi/2) + (\xi^3/24)]\}. \quad (2)$$

In Eq. (2), $\mathrm{Ai}(x)$ represents the Airy function, $\eta = s - (\varepsilon\xi^2/4)$, E_0 is peak field amplitude, and $\varepsilon = \pm 1$ depending on the sign of r_{eff}. In the above expression, the coordinates have been normalized, e.g., $s = x/x_0$ and $\xi = z/(kx_0{}^2)$, where x_0 is an arbitrary spatial scale. Note that this Airy self-localized wave is exponentially truncated with a decay coefficient $\gamma = k^2 n^2 x_0 r_{\text{eff}} k_B T/(2e)$, and thus conveys finite power. It is also evident that this asymmetric wave packet propagates without any change (in spite of diffraction effects) while it continuously self-bends during propagation at a rate $\xi^2/4$ that is independent of $k_B T$.

In the linear case ($\gamma = 0$), the solution reduces to a simple, infinitely extended Airy function, first obtained in Ref. [4]. In the nonlinear, truncated case ($\gamma \neq 0$), Eq. (2) indicates that these asymmetric and diffraction-free properties are retained, with invariant propagation arising from diffusion effects. Interestingly, this self-trapping is due to irreversible transverse energy flow, which in turn explains the large asymmetry in the beam's intensity profile.

In the paraxial domain, the transverse Poynting vector is given by $\vec{S}_\perp = i\hat{x}(4\eta_0 k)^{-1}(EE_x^* - E^* E_x)$ where $E_x = \partial E/\partial x$ [20,21]. Figure 1(a) depicts the intensity profile of a diffusion-trapped Airy state during propagation when the photorefractive decay factor $\gamma = 0.12$. The arrows in the figure, indicating the lateral power flow density, all point toward the direction of deflection. In addition, their magnitude increases linearly with distance, showing that the beam constantly accelerates as it propagates, so as to keep up with displacement of the beam's centroid $\langle s_c \rangle$. Indeed, it can be shown from Eq. (2) that the centroid path is characterized by the parabola:

$$\langle s_c \rangle = \frac{1}{8\gamma} + \varepsilon\frac{\xi^2}{4}. \quad (3)$$

The propagation of this same beam in the linear case (without material charge diffusion) is shown in Fig. 1(b). In this case, because of the high initial confinement, the intensity features of the beam continuously broaden during propagation. This is also apparent in the direction of the transverse flow. In this regime, the arrows point in both directions, so as to allow the centroid to move along a straight line [22]. For the case of a reverse phase chirp [$s \rightarrow -s$ in Eq. (2)], the phase acceleration is in the same direction as diffusive transport, and the beam loses its Airy profile [Fig. 1(c)]. Again, power flows in both directions, though with a more complex pattern than in the linear, purely diffractive case.

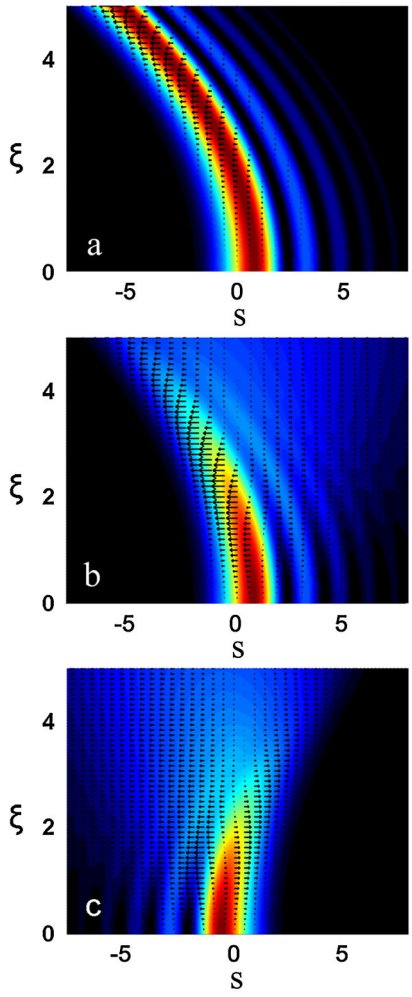

FIG. 1 (color online). Transverse energy power flow. (a) The intensity profile of a self-trapped Airy state during propagation when the photorefractive decay factor is present. (b, c) The propagation of this same beam (b) in the absence of diffusion and (c) when the phase profile is reversed.

The exponental truncation $\exp(-2\gamma\eta)$ contributes greatly to the experimental ease of production. The impact of this is seen most clearly by Fourier transforming Eq. (2), which gives $\Phi(K) \sim \exp(-AK^2)\exp(iK^3/3)$, where A is a constant proportional to γ [2]. This is simply a Gaussian spectrum modulated with a cubic phase.

Experimental confirmation of Eq. (2) was performed using 532 nm continuous wave laser light projected onto an $8 \times 8 \times 8$ mm SBN:75 crystal. The setup is shown in Fig. 2. The creation of the truncated Airy beam consists of three basic steps: (1) an initial Gaussian beam is projected onto a spatial light modulator (SLM), (2) a cubic phase chirp is impressed upon the beam, to create $\Phi(K)$, and (3) the beam is Fourier transformed by a cylindrical lens to generate the incident Airy beam $E(x)$. A wave plate is used to adjust the polarization of this beam with respect to the crystalline axis. For SBN:75, $r_{33} = 1340$ pm/V and $r_{13} = 67$ pm/V, so that the index change above the base index $n_0 = 2.3$ depends on the polarization (for fixed tempera-

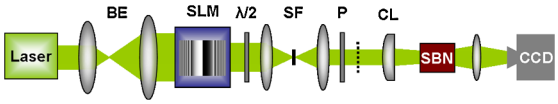

FIG. 2 (color online). Experimental setup. Light from a 532 nm laser is expanded and phase-modulated by a spatial light modulator (SLM). The beam is Fourier transformed by a cylindrical lens and input into an SBN:75 photorefractive crystal. Light exiting the crystal is imaged into a CCD camera. BE, beam expander; $\lambda/2$, half-wave plate; SF, spatial filter; P, polarizer; CL, cylindrical lens; dashed line, SLM image plane.

ture). For the experiments, we take advantage of the anisotropy and use ordinary polarization as a near-linear reference beam for comparison with extraordinary polarization. Finally, at the exit face of the crystal, the output is imaged into a CCD camera.

Typical experimental and numerical results are shown in Fig. 3. The input Airy beam is roughly 100 μm wide and contains 350 mW of power. For extraordinary polarization [Figs. 3(a)–3(f)], the beam maintains its profile as it propagates. There is no diffraction, particularly evident in the main lobe, with a transverse displacement of 32 μm at the output. The dependence of diffusion trapping on polarization provides unequivocal verification of its nonlinear origins. For ordinary polarization [Figs. 3(g)–3(l)], propagation is essentially linear and the beam diffracts. The sizes of both the beam and its central lobe roughly

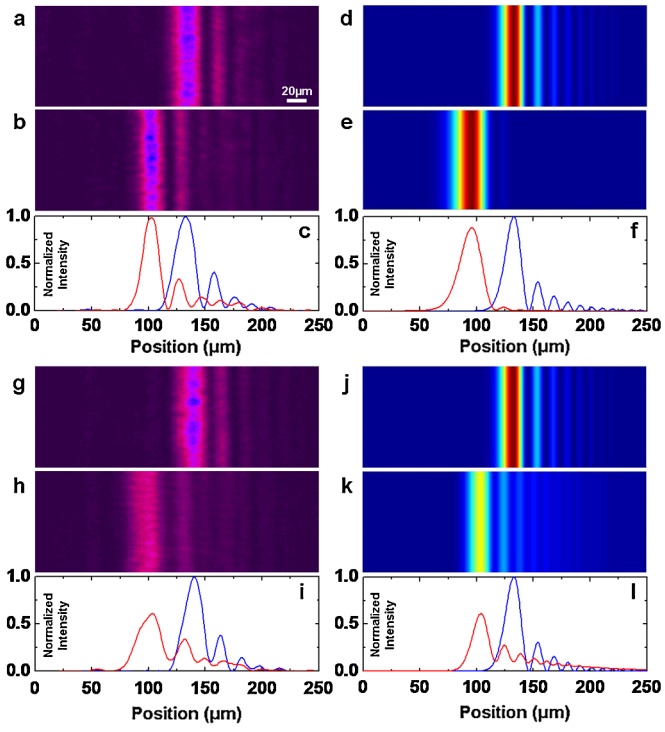

FIG. 3 (color online). Nonlinear Airy beam propagation for a 350 mW beam with (a–f) extraordinary and (g–l) ordinary polarization. (a, d, g, j) are inputs, (b, e, h, k) are outputs, and (c, f, i, l) are cross sections. Left column, experiments; right column, simulations.

double after 8 mm of propagation, with the central lobe curving by 37 μm from the initial center line. By comparison, a Gaussian beam with the same 20 μm FWHM of the central lobe (not shown) would diffract by 5 times and propagate straight.

Another test of linear vs nonlinear propagation arises from the slow nature of the photorefractive response. This is shown in Fig. 4, in which we observe the nonlinear output for the extraordinarily polarized Airy beam as a function of time. At first, charges have been photoexcited but have not yet diffused, so the output beam exhibits pure diffraction. As time evolves, the diffusive PR nonlinearity becomes more pronounced, gradually bringing the beam back to a nondiffracted state. As shown in Figs. 4(b)–4(f), the lobes focus and narrow, with the first lobe shifting to the right over time and the second (and higher) lobes shifting left. This final state, akin to that in Fig. 3(h), follows from the relative phase shift between neighboring lobes and, more generally, conforms to Ehrenfest's theorem on the conservation of mass (light intensity) during propagation.

Without the nonlinear term in Eq. (1), the dynamics are symmetric with respect to transverse orientation. For example, left-leaning and right-leaning Airy beams propagate identically in linear media (except for the reversal of acceleration). In the unbiased photorefractive, however, the reversed profile is not a solution. This is shown in Fig. 5, where we have created a mirror-opposite beam by reversing the phase mask on the SLM. In this case, the asymmetry of the cubic phase chirp is in the same direction as the nonlinear asymmetry provided by the crystalline c axis. Beam acceleration and two-wave mixing therefore operate

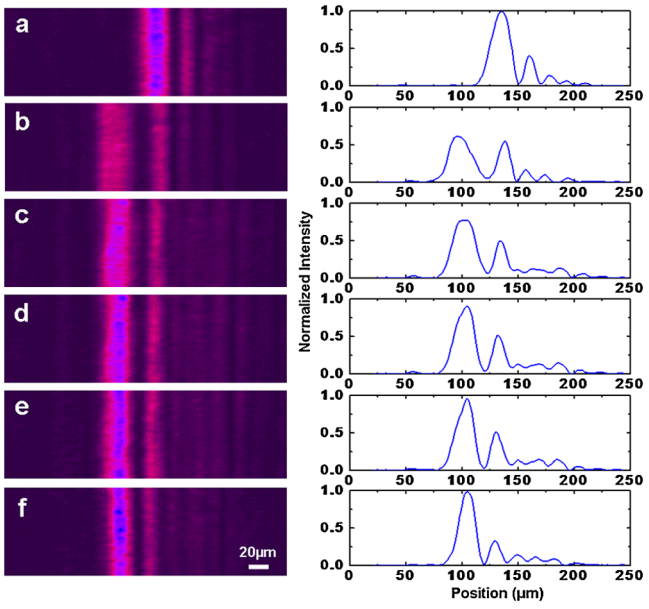

FIG. 4 (color online). Time evolution of diffusive process for the Airy beam in Fig. 3(b). (a) Input and (b–f) output. (b–f) are recorded every 20 seconds. Left column, experimental pictures; right column, cross sections.

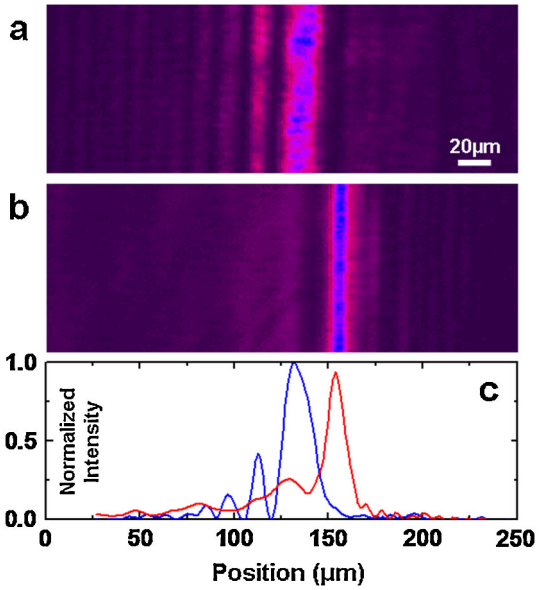

FIG. 5 (color online). Reversed Airy beam propagation. Experimental pictures for (a) input, (b) output, and the corresponding (c) cross sections.

in the same direction, compressing the main peak and removing the side lobes. Simulations show that for longer propagation distances, the momentum transfer continues, causing intensity overshoot and enhanced diffraction of the beam.

Remarkably, the balance between diffraction and nonlinearity does not depend on the intensity of the initial Airy beam (as it does for other self-trapped beams, such as solitons) [10]. Since two-wave mixing depends on the gradient, rather than the strength, of the intensity, the peak field amplitude E_0 appears only as an independent scaling parameter in the solution (2). This is confirmed experimentally in Fig. 6, which shows extraordinary Airy propagation for beams with different initial input powers 200 mW [6(a)] and 500 mW [6(b)]. As shown in Figs. 6(b), 6(c), and 6(e), and 6(f), as well as the 350 mW case in Fig. 3(b), the outputs have nearly identical profiles, with the same

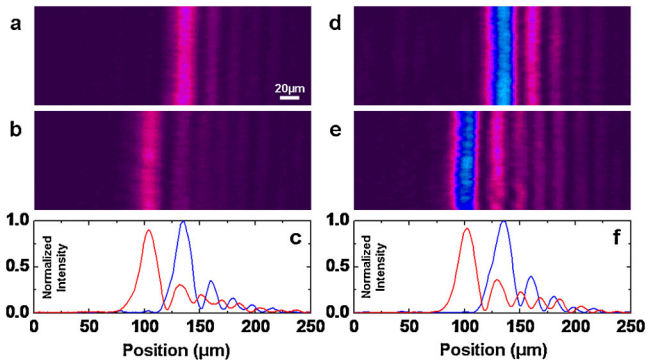

FIG. 6 (color online). Nonlinear Airy beam propagation with different input powers (a, b, c) 0.2 W and (d, e, f) 0.5 W. Top row, input; middle row, output; bottom row, cross sections.

transverse displacement of 32 μm, while experiencing no diffraction during propagation. This independence of intensity makes such beams promising for nonlinear applications, such as sorting and trapping in colloids [23] and imaging using spatial nonlinearity [24].

In summary, we have observed the propagation of a finite-energy Airy beam in an unbiased photorefractive medium. The results are the first example of solitary-like wave formation using two-wave mixing and, more generally, demonstrate that the dynamics arising from an asymmetric phase chirp can be counteracted by an asymmetric nonlinearity.

[1] G. A. Siviloglou and D. N. Christodoulides, Opt. Lett. **32**, 979 (2007).
[2] G. A. Siviloglou, J. Broky, A. Dogariu, and D. N. Christodoulides, Phys. Rev. Lett. **99**, 213901 (2007).
[3] J. Durnin, J. Opt. Soc. Am. A **4**, 651 (1987); J. Durnin, J. J. Miceli, and J. H. Eberly, Phys. Rev. Lett. **58**, 1499 (1987).
[4] M. V. Berry and N. L. Balazs, Am. J. Phys. **47**, 264 (1979).
[5] J. Baumgartl, M. Mazilu, and K. Dholakia, Nat. Photon. **2**, 675 (2008).
[6] P. Polynkin *et al.*, Science **324**, 229 (2009).
[7] M. Asorey, P. Facchi, V. I. Man'ko, G. Marmo, S. Pascazio, and E. C. G. Sudarshan, Phys. Rev. A **77**, 042115 (2008).
[8] T. Ellenbogen, N. Voloch-Bloch, A. Ganany-Padowicz, and A. Arie, Nat. Photon. **3**, 395 (2009).
[9] Y. R. Shen, *Principles of Nonlinear Optics* (Wiley & Sons, New York, 1984).
[10] M. Segev, B. Crosignani, A. Yariv, and B. Fischer, Phys. Rev. Lett. **68**, 923 (1992).
[11] M. Segev *et al.*, Phys. Rev. Lett. **73**, 3211 (1994).
[12] D. N. Christodoulides and M. I. Carvalho, J. Opt. Soc. Am. B **12**, 1628 (1995).
[13] G. C. Valley *et al.*, Phys. Rev. A **50**, R4457 (1994).
[14] M. Taya *et al.*, Phys. Rev. A **52**, 3095 (1995).
[15] N. Kukhtarev *et al.*, Ferroelectrics **22**, 949 (1979).
[16] M. Segev, Y. Ophir, and B. Fischer, Opt. Commun. **77**, 265 (1990).
[17] O. V. Lyubomudrov and V. V. Shkunov, J. Opt. Soc. Am. B **11**, 1403 (1994).
[18] D. N. Christodoulides and M. I. Carvalho, Opt. Lett. **19**, 1714 (1994).
[19] D. N. Christodoulides and T. H. Coskun, Opt. Lett. **21**, 1460 (1996).
[20] J. Broky *et al.*, Opt. Express **16**, 12 880 (2008).
[21] H. I. Sztul and R. R. Alfano, Opt. Express **16**, 9411 (2008).
[22] I. M. Besieris and A. M. Shaarawi, Opt. Lett. **32**, 2447 (2007); G. A. Siviloglou, J. Broky, A. Dogariu, and D. N. Christodoulides, *ibid.* **33**, 207 (2008).
[23] W. M. Lee, R. El-Ganainy, D. N. Christodoulides, K. Dholakia, and E. M. Wright, Opt. Express **17**, 10 277 (2009).
[24] C. Barsi, W. Wan, and J. W. Fleischer, Nat. Photon. **3**, 211 (2009).